NASA/TM—2018-219872

Magnetic Properties of Fe-49Co-2V alloy and pure Fe at Room and Elevated Temperatures

Henry C. de Groh III and Steven M. Geng
Glenn Research Center, Cleveland, Ohio

Janis M. Niedra
ASRC Aerospace Corporation, Cleveland, Ohio

Richard R. Hofer
Jet Propulsion Laboratory, Pasadena, California

April 2018

NASA STI Program . . . in Profile

Since its founding, NASA has been dedicated to the advancement of aeronautics and space science. The NASA Scientific and Technical Information (STI) Program plays a key part in helping NASA maintain this important role.

The NASA STI Program operates under the auspices of the Agency Chief Information Officer. It collects, organizes, provides for archiving, and disseminates NASA's STI. The NASA STI Program provides access to the NASA Technical Report Server—Registered (NTRS Reg) and NASA Technical Report Server—Public (NTRS) thus providing one of the largest collections of aeronautical and space science STI in the world. Results are published in both non-NASA channels and by NASA in the NASA STI Report Series, which includes the following report types:

- TECHNICAL PUBLICATION. Reports of completed research or a major significant phase of research that present the results of NASA programs and include extensive data or theoretical analysis. Includes compilations of significant scientific and technical data and information deemed to be of continuing reference value. NASA counter-part of peer-reviewed formal professional papers, but has less stringent limitations on manuscript length and extent of graphic presentations.

- TECHNICAL MEMORANDUM. Scientific and technical findings that are preliminary or of specialized interest, e.g., "quick-release" reports, working papers, and bibliographies that contain minimal annotation. Does not contain extensive analysis.

- CONTRACTOR REPORT. Scientific and technical findings by NASA-sponsored contractors and grantees.

- CONFERENCE PUBLICATION. Collected papers from scientific and technical conferences, symposia, seminars, or other meetings sponsored or co-sponsored by NASA.

- SPECIAL PUBLICATION. Scientific, technical, or historical information from NASA programs, projects, and missions, often concerned with subjects having substantial public interest.

- TECHNICAL TRANSLATION. English-language translations of foreign scientific and technical material pertinent to NASA's mission.

For more information about the NASA STI program, see the following:

- Access the NASA STI program home page at http://www.sti.nasa.gov

- E-mail your question to help@sti.nasa.gov

- Fax your question to the NASA STI Information Desk at 757-864-6500

- Telephone the NASA STI Information Desk at 757-864-9658

- Write to:
  NASA STI Program
  Mail Stop 148
  NASA Langley Research Center
  Hampton, VA 23681-2199

NASA/TM—2018-219872

Magnetic Properties of Fe-49Co-2V alloy and pure Fe at Room and Elevated Temperatures

Henry C. de Groh III and Steven M. Geng
Glenn Research Center, Cleveland, Ohio

Janis M. Niedra
ASRC Aerospace Corporation, Cleveland, Ohio

Richard R. Hofer
Jet Propulsion Laboratory, Pasadena, California

National Aeronautics and
Space Administration

Glenn Research Center
Cleveland, Ohio 44135

April 2018

Acknowledgments

Portions of the research described in this paper were carried out at the Jet Propulsion Laboratory, California Institute of Technology, under a contract with the National Aeronautics and Space Administration.

Level of Review: This material has been technically reviewed by technical management.

Available from

NASA STI Program
Mail Stop 148
NASA Langley Research Center
Hampton, VA 23681-2199

National Technical Information Service
5285 Port Royal Road
Springfield, VA 22161
703-605-6000

This report is available in electronic form at http://www.sti.nasa.gov/ and http://ntrs.nasa.gov/

Magnetic Properties of Fe-49Co-2V alloy and pure Fe at Room and Elevated Temperatures

Henry C. de Groh III and Steven M. Geng
National Aeronautics and Space Administration
Glenn Research Center
Cleveland, Ohio 44135

Janis M. Niedra*
ASRC Aerospace Corporation
Cleveland, Ohio 44135

Richard R. Hofer
Jet Propulsion Laboratory
Pasadena, California 91109

Abstract

The National Aeronautics and Space Administration (NASA) has a need for soft magnetic materials for fission power and ion propulsion systems. In this work the magnetic properties of the soft magnetic materials Hiperco 50 (Fe-49wt%Cr-2V) and CMI-C (commercially pure magnetic iron) were examined at various temperatures up to 600 °C. Toroidal Hiperco 50 samples were made from stacks of 0.35 mm thick sheet, toroidal CMI-C specimens were machined out of solid bar stock, and both were heat treated prior to testing. The magnetic properties of a Hiperco 50 sample were measured at various temperatures up to 600 °C and then again after returning to room temperature; the magnetic properties of CMI-C were tested at temperatures up to 400 °C. For Hiperco 50 coercivity decreased as temperature increased, and remained low upon returning to room temperature; maximum permeability improved (increased) with increasing temperature and was dramatically improved upon returning to room temperature; remanence was not significantly affected by temperature; flux density at H = 0.1 kA/m increased slightly with increasing temperature, and was about 20% higher upon returning to room temperature; flux density at H = 0.5 kA/m was insensitive to temperature. It appears that the properties of Hiperco 50 improved with increasing temperature due to grain growth. There was no significant magnetic property difference between annealed and aged CMI-C iron material; permeability tended to decrease with increasing temperature; the approximate decline in the permeability at 400 °C compared to room temperature was 30%; saturation flux density, B_S, was approximately equal for all temperatures below 400 °C; B_S was lower at 400 °C.

Background

Applications

This work was done in support of the development of two NASA systems: an annular linear induction pump to be used in a 40 $kW_{(electrical)}$ fission power system (FPS); and for soft magnetic parts used in the construction of Hall thruster ion propulsion systems.

*Retired.

Annular Linear Induction Pump

Fission power systems (FPS) are being developed to provide electricity for planetary surface missions (Ref. 1). A key component of this power system is the annular linear induction pump (ALIP) (Ref. 2). The ALIP is used to circulate liquid sodium-potassium- (NaK-78) to transfer heat from a nuclear reactor to several free-piston Stirling power convertors (Refs. 3 and 4). The ALIP uses stator laminations made of an Fe-49% Co-2% V alloy with the trade name Hiperco 50 to generate a moving magnetic field that applies a magnetic force on the NaK-78 fluid (Ref. 5). Hiperco 50 has 0.01% C and 0.05% Nb added for grain refinement. The Idaho National Lab designed and built an ALIP for NASA. Upon testing, the ALIP did not perform as expected. Based on magnetic finite element analysis (FEA) of the pump, it was concluded that the assumed Hiperco 50 magnetic properties at the pump operating temperatures (550 °C) might be a part of the problem. High temperature magnetic flux density as a function of magnetic field intensity (B-H) data for Hiperco 50 could not be found in the open literature. The purpose of this work was to measure the magnetic properties of Hiperco 50 at temperatures up to 600 °C, so that the ALIP could be more accurately modeled. These data are also needed for proper modeling and design of the Hall thruster which uses Hiperco 50A in some sections of its magnetic circuit.

Hall Thruster

A Hall thruster is a type of in-space propulsion system used in orbit raising, stationkeeping, and deep space applications (Refs. 6 and 7). Electric and magnetic fields are used in Hall thrusters to ionize and accelerate a working gas, typically xenon, to exhaust velocities of 10 to 30 km/s. A variety of materials are used in the thruster depending on the application requirements. Two of those materials are: Hiperco 50A which is an Fe-49% Co-2% V alloy (0% C and Nb) (Ref. 8); and CMI-C which is a low-carbon electromagnetic iron from CMI Specialty Products (Chesire, CT). Hiperco 50A is used in areas were magnetic property demands are the highest. CMI-C is used in areas where magnetic performance requirements are moderate. The performance of the thruster depends on the magnetic properties of Hiperco 50A and CMI-C, thus the magnetic properties of these materials must be known so the thruster can be properly designed. The maximum operating temperatures of the magnetic circuit components in a Hall Thruster are typically near 400 °C, thus the magnetic properties of Hiperco 50A and CMI-C at this temperature are needed. In this memorandum we report measurements made of the magnetic properties of Hiperco 50 and CMI-C at elevated temperatures. Since the nominal composition of Hiperco 50 and 50A are the same, it is expected that their magnetic properties will behave similarly at elevated temperatures. Confirmation of this will be explored in future work.

Metallurgical Background

The favorable magnetic properties of Fe-50Co alloys were first noted by Elmen (Ref. 9). Stanley and Yensen (Ref. 10) found that 0.5% Cr additions to Fe-35%Co improved ductility; the resulting alloy was named Hiperco. Carpenter Technology Corp. developed Hiperco 50 with the addition of 2% V and 0.05% Nb. Niobium additions added strength but resulted in lower permeability and higher coercivity. Hiperco 50A has no Nb. Both Hiperco 50 and 50A have trace amounts of Mn, and Si. The Hall thruster parts for which this alloy is being used are not under significant loads, however high permeability and saturation, and low coercivity are required, thus Hiperco 50A was selected.

In general, according to Reference 11, after melting and casting Fe, Co, and V into an ingot, the ingot is hot-rolled above the alpha-gamma transformation temperature (>925 °C). The alpha-gamma transformation temperature is the boundary between the two phases which can be seen in Figure 1 in the Fe-Co phase diagram. It should be noted that the addition of 2% V lowers the alpha-gamma transformation temperature to about 880 °C (Ref. 11). The alloy is hot-rolled because the ductility of the disordered gamma phase is higher. Then an anneal at 850 °C is imposed to form the alpha structure needed for the development of good magnetic properties in the final part. The higher temperature alpha

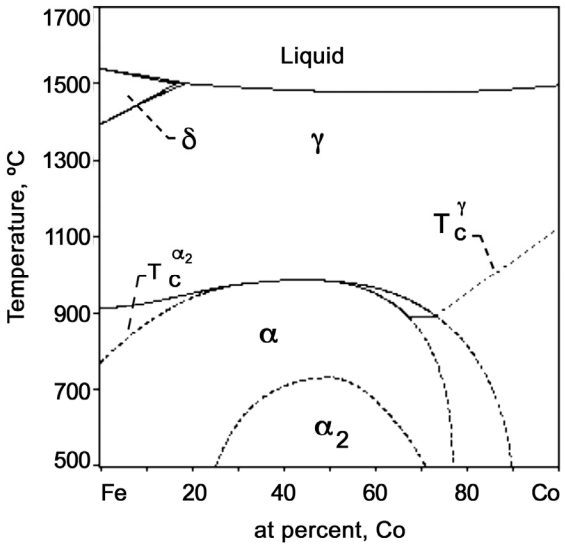

Figure 1.—Fe-Co phase diagram.

phase is disordered bcc (body-centered cubic); below 730 °C the bcc alpha phase undergoes an atomic ordering to a CsCl structure-type (Refs. 11 and 12). The disordered alpha phase is more ductile, and the formation of the ordered phase can be suppressed by quenching from above 730 °C. Thus if the material is going to be cold rolled into sheets, it is quenched from the 850 °C anneal temperature (Ref. 11). Hiperco 50A is frequently used in laminate stator core applications in electric motors and generators; in such applications the laminates are cold rolled to thicknesses of the order of 0.2 mm (Refs. 13 and 14). After cold rolling, the magnetic properties of the material are poor due to the resulting fine grain structure; heat treatment is needed to recrystallize and grow the grain structure there-by optimizing the magnetic properties (Ref. 15). To develop high flux density at relatively low applied field the final heat treatment is done between 650 and 875 °C with the lower temperatures used when high strength and ductility are needed and the higher temperatures used to optimize magnetic properties. The order/disorder reaction that takes place during cooling from the anneal temperature strongly affects permeability and coercivity. It has been established that permeability can be maximized, and coercive force minimized by employment of a moderate cooling rate of between 100 and 250 °C/h (Refs. 8, 11, 16, and 17). In Fe-49Co-2V work by Jusso it was shown that slow cooling (25 °C/h) and fast cooling (10,000 °C/h) resulted in 3x to 5x lowering of permeability, and a 2x increase in coercive force compared to 250 °C/h cooling (Ref. 16). Low magnetocrystalline anisotropy is needed for soft magnetic materials (high permeability and low coercivity) and ordering has a marked effect on anisotropy which is minimized at an intermediate degree of ordering; this is thought to be the reason why a moderate cooling rate helps optimize magnetic properties in Fe-Co-2V alloys (Ref. 16). Current literature recommends cooling rates of 150 °C/h and 55 to 78 °C/h for Hiperco 50A and CMI-C respectively (Refs. 8, 11, 18, 19, 20, 21, and 22). Recall that slower is not necessarily better for Hiperco 50A because the moderate cooling rate is balancing grain growth and the relative amounts of ordered and disordered phases. Future work is expected to include determination of optimum heat treatments for Hiperco 50A and pure core iron; it should also be noted that the heat treatment could be optimized for the magnetic properties at some temperature other than room temperature.

Prior Work

Horwath et al. made high temperature magnetic property measurements of three Fe-Co alloys including Hiperco 50 (Ref. 23). For Hiperco 50 heat treated for 45 min at 730 °C, they observed an initial decrease in coercivity during aging at 500 °C, and a doubling after 5000 h at 500 °C. These data are

valuable, however, we need data for material subjected to different heat treatments (in the range of 816 to 870 °C), with magnetic properties measured using DC, which include B_s (saturation flux density) and permeability. Li examined the magnetic properties of Hiperco 50 (after being heat treated in dry hydrogen at 760 °C for 2 h and cooled at 180 °C/h) at temperatures up to 800 °C (Ref. 24). Li observed decreases of 10% and 35% in flux density and coercivity respectively with increasing temperature up to 580 °C; aging for 1150 h at 450 °C caused a 20% decline in flux density (at H = 10 Oe) and permeability and no change in coercivity. The heat treatment Li used was significantly different from the heat treatment commonly recommended in the literature (Ref. 18); thus although the absolute value of properties at temperature may not be universally applicable, the trends Li observed may still be pertinent. Kueser et al. evaluated the properties of eight magnetic materials for use at high temperatures (up to 593 °C), including Hiperco 50 and Supermendur (Supermendur has the same nominal composition as Hiperco 50 but is said to have higher resistivity, and thus lower losses when used with alternating current) (Ref. 25). The details of the stress-relief anneal imposed on the 0.02 cm thick laminations tested by Kueser were not provided, however, DC B_s and AC core losses decreased approximately 5% and 7%, respectively upon heating from room temperature to 427 °C. A review of FeCo alloys was presented by Sundar and Deevi (Ref. 26). Bogma compared the magnetic properties of stoichiometric FeCo as a function of temperature and degree of α-phase order and found the saturation induction of the ordered phase to be 2 to 3% higher than in the disordered state (Ref. 27).

Morishita et al. examined the magnetic properties of several irons (including SPCC which is nearly pure iron with small amounts of C, Mn, P, and S) at temperatures up to 700 °C using alternating current at 50 Hz (Ref. 23). They found that SPCC saturation flux density (B_s) remained constant up to approximately 550 °C; permeability increased with temperature; and iron core losses decreased with increasing temperature. These results are somewhat expected since it is know that lattice distortions interfere with the movement of magnetic domains and that losses decrease with increasing grain size (Ref. 28). As temperature is increased, lattice distortions are expected to decline, and grain size increase. The lower electrical conductivity of iron (SPCC) at higher temperatures also contributes to low alternating current losses as temperature is increased (Ref. 29). These trends are valuable, however do not satisfy our need for ASTM standard direct current (DC) magnetic property data with relevant heat treatments.

Experimental Procedure

Hiperco 50 Testing

A Hiperco test article was prepared for this test as shown in Figure 2. The test article contains a stack of (quantity thirty) Hiperco 50 rings that were annealed in hydrogen at 843 to 871 °C for 2 to 4 h; cooled at 83 to 194 °C/h to 316 °C, then at any rate to room temperature. After annealing, an oxide coating was added by heating in air at 480 °C for approximately 60 min. The approximate dimensions of the rings were: ID = 1.955 in., OD = 2.571 in., and thickness = 0.014 in. The Hiperco test article was equipped with an excitation coil for introducing a magnetic field to the Hiperco material, and a sensing coil for

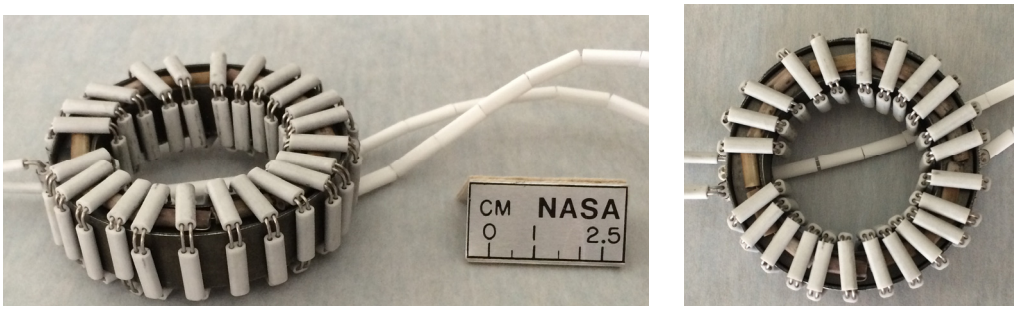

Figure 2.—Hiperco 50 test article equipped with excitation and sensing coils.

measuring the resulting magnetic flux density. Both the excitation coil and the sensing coil were made of 20-gauge Nickel 201. Two type-K thermocouples were mounted to the ring canister for monitoring temperature. The type-K thermocouples consisted of 24-gauge chromel and alumel wires.

A custom built hysteresigraph, as shown in Figure 3, was used to provide electrical current to the excitation coil, and to measure the resultant flux density in the Hiperco rings. An AC voltage was applied to the excitation coil between measurements to degauss the test article. The test was conducted in a Pereco model MTX427 furnace, and in an inert environment (Argon cover gas). An Agilent data logger was used to record the test data. A schematic drawing of the test set-up is shown in Figure 4, while Figure 5 is a photograph of the actual test set-up.

Figure 3.—Hysteresigraph.

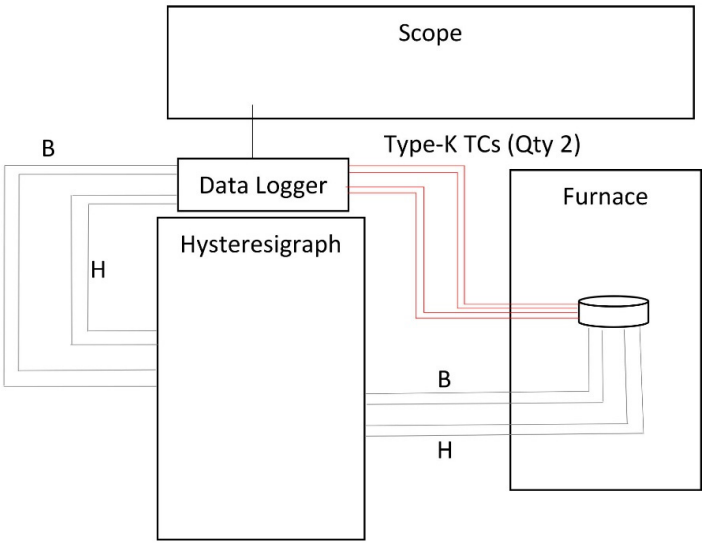

Figure 4.—Schematic of test set-up.

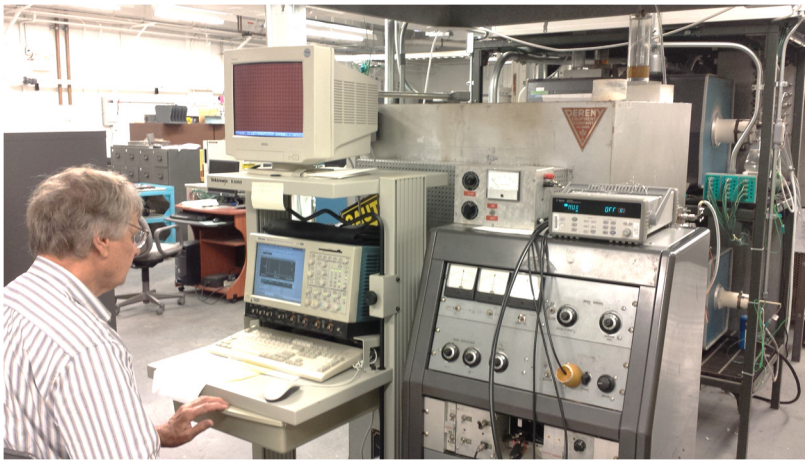

Figure 5.—Test set-up in lab.

Test Matrix

The B-H properties of Hiperco 50 were measured at various temperatures, from room temperature, up to 600 °C in increments of mainly 100 °C. A 550 °C data point was also recorded since that is the operating temperature of the ALIP. After the 600 °C data point was recorded, the test article was returned to 23 °C, and the BH properties re-measured to check for oxidation of the Hiperco rings. Data were recorded once the test article reached steady-state temperature. A typical measurement took about 90 sec to complete.

CMI-C Testing

An example of low-carbon magnetic iron is CMI-C Electromagnetic Iron from CMI Specialty Products (Chesire, CT). This material conforms to ASTM A848-01, "Standard Specification for Low-Carbon Magnetic Iron." In order to confirm the performance of the CMI-C iron, DC magnetic testing of the material was conducted. This testing was performed by KJS Associates (Indianapolis, IN) in compliance with ASTM A773/A773M-01, "Standard Test Method for D-C Magnetic Properties of Materials Using Ring and Permeameter Procedures with D-C Electronic Hysteresigraphs." The vendor reports an uncertainty of approximately ±1% for B (resulting magnetic flux density) and H (imposed magnetic field intensity).

Three magnetic samples were sent to KJS for testing. The samples were machined from a 2 in. (5.08 cm) outer diameter rod of CMI-C provided by CMI. The samples were machined to the dimensions shown in Figure 6 and were prepared according to Table 1. The "Raw" sample was not subjected to any aging or annealing, it was the "as-received" state provided by CMI. The "Aged" sample was first annealed and then aged at 204 °C for 4 h. The "Annealed" sample was annealed, with no aging. Both the Aged and Annealed samples were annealed together in a vacuum atmosphere at 843 °C for 4 h, cooled at 56 to 111 °C per hour until the temperature reached 510 °C and then cooled at the furnace rate without quenching. Testing was conducted at 25 °C for all three samples. The annealed sample was also subjected to testing at temperatures of 100, 200, 300, and 400 °C. Hall thruster magnetic circuits typically operate at temperatures of 200 to 400 °C.

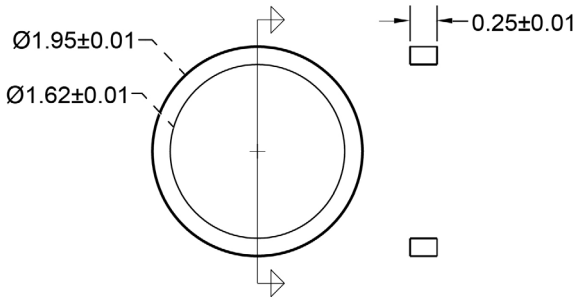

Figure 6.—Dimensions in inches of the CMI-C magnetic samples.

TABLE 1.—CMI-C SAMPLE DESCRIPTIONS

Sample name	Preparation	Test temperatures, °C
Raw	None, As-received	25
Aged	Annealed then aged for 4 h at 204 °C (400 °F)	25
Annealed	4 h Anneal at 843 °C	25, 100, 200, 300, 400

Results

Hiperco 50

The magnetic properties of a Hiperco 50 stacked lamination ring sample were tested at various elevated temperatures up to 600 °C, then tested again after returning back to 21 C. Hiperco 50 is the same as Hiperco 50A except Hiperco 50 has 0.05% Nb and 0.01% C added to improve strength after annealing. The laminated ring sample was annealed at 816 °C prior to testing. The Hiperco BH properties recorded during these tests are shown in Figures 7 to 15.

The data were analyzed; Table 2 and Figure 16 summarize the results. Coercivity decreased as temperature increased, and remained low upon returning to room temperature, presumably due to further grain growth as temperature was increased. The maximum permeability was determined by the maximum slope of a line drawn through the origin and the initial magnetization curve. Relative permeability was determined by dividing by the permeability of vacuum $\mu_o = 1.2566\times10^{-6}$ H/m ($4\pi\times10^{-7}$). The remanence value was where the demagnetization curve crossed the vertical (B) axis. The flux density at H equals 0.1 kA/m (1.25 Oe, Figure 16) and H = 0.5 kA/m (6.25 Oe, Table 2) were the magnetic flux densities resulting in the sample due to the imposed H field of 0.1 or 0.5 kA/m, read off of the magnetization curve. Permeability improved (increased) with increasing temperature and was dramatically improved upon returning to room temperature. Remanence was not significantly affected by temperature. Flux density at H = 0.1 kA/m increased slightly with increasing temperature, and was about 20% higher upon returning to room temperature. Flux density at H = 0.5 kA/m was insensitive to temperature. Since magnetic properties are influenced by grain structure, it appears from the data that the grain structure of the material changed at the higher test temperatures, particularly at temperatures equal to and greater than 500 °C. Coercivity and permeability improved substantially at these higher temperatures as the grain structure improved due to inferred grain growth. The larger grains of course remained upon return to room temperature.

The decrease in coercivity at higher temperatures was also observed by Fingers (Ref. 30) who did an aging study at 500 °C. However, Fingers also found that after this initial decrease, the coercivity of Hiperco 50 increased with additional time at 500 °C, increasing and stabilizing at about 16% above initial values after 2000 h. Permeability was not included in Fingers' study.

The B-H hysteresis loops appear similar to those reported previously in Reference 31 at 600 to 700 °C, for the core exposed to about 1000 °C and its magnetic anneal lost. The onset of the anomalous Barkhausen effect (Ref. 32) can be made out in the initial magnetization curve in Figure 14 (600 °C) as jiggles in the line. Its presence is not surprising, since the two materials are quite similar, with Supermendur having a reduced level of undesirable impurities, as for example carbon. No further effort was expended on this in the present study, such as by slowing down the dB/dt rate to emphasize the effects of the magnetic viscosity field.

TABLE 2.—MAGNETIC PROPERTIES OF HIPERCO 50 AT VARIOUS TEMPERATURES

	Temperature, °C								
Property	21	100	200	300	400	500	550	600	Return to 21
Coercivity, Oe	1.137	1.113	1.114	1.063	0.970	0.781	0.616	0.567	0.567
Max relative permeability	14,553	13,361	12,998	12,271	13,589	17,715	19,845	22,051	30,513
Retentivity, G	12,400	11,400	11,700	11,000	11,300	11,000	11,500	12,600	12,300
B at H = 0.1 kA/m (1.25 Oe), G	10,650	10,500	10,700	10,000	10,700	11,100	12,100	12,000	12,600
B at 0.5 kA/m, G	17,300	16,500	16,800	16,100	16,600	16,800	17,200	16,800	18,600

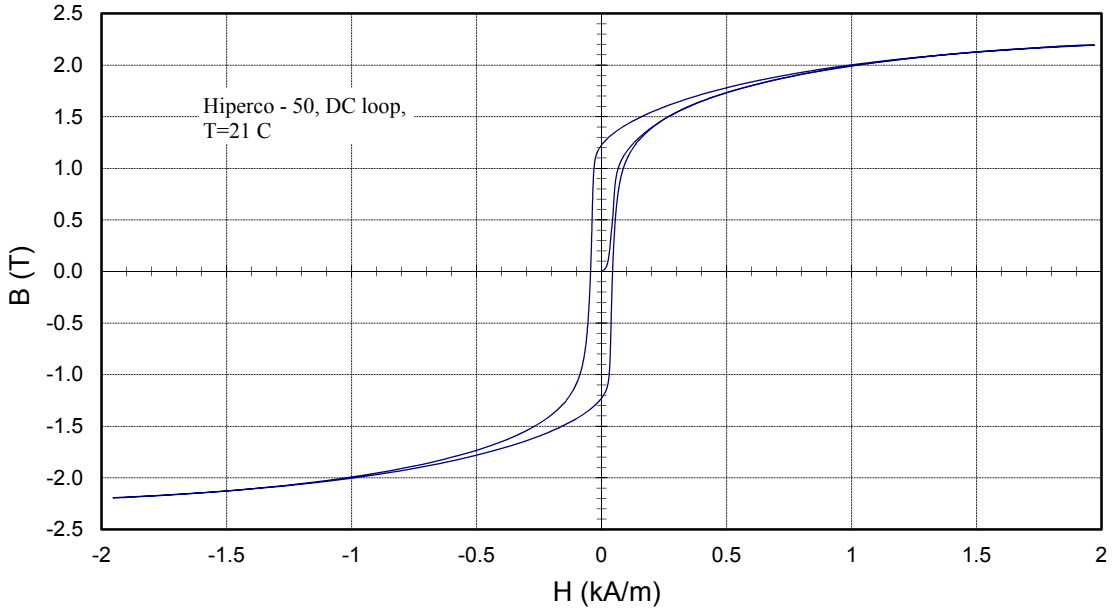

Figure 7.—Initial direct current BH properties of Hiperco 50 at room temperature (23 °C).

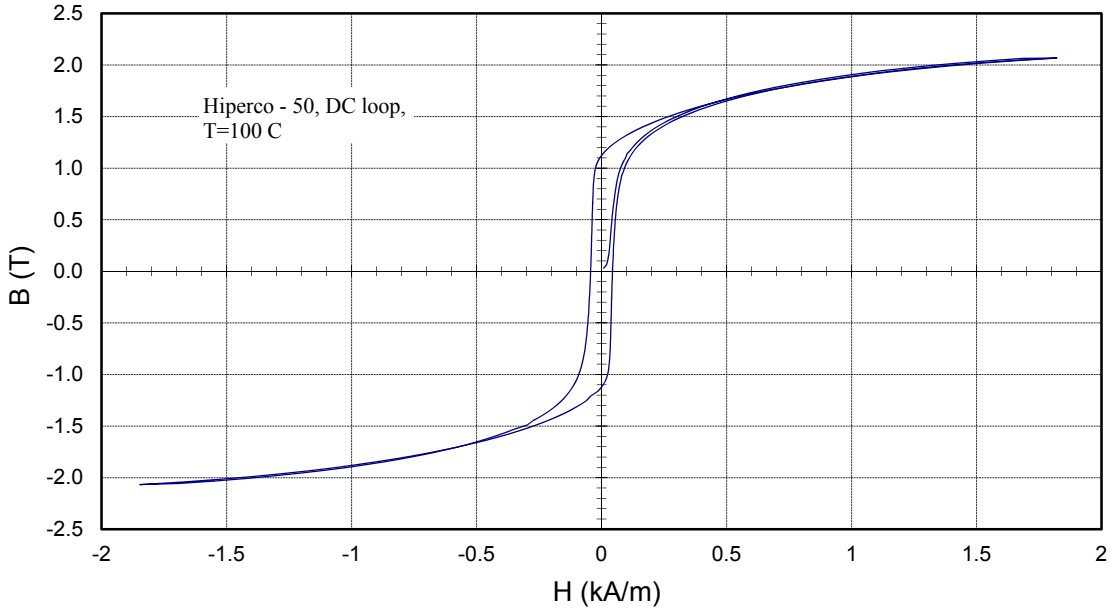

Figure 8.—Direct current BH properties of Hiperco 50 at 100 °C.

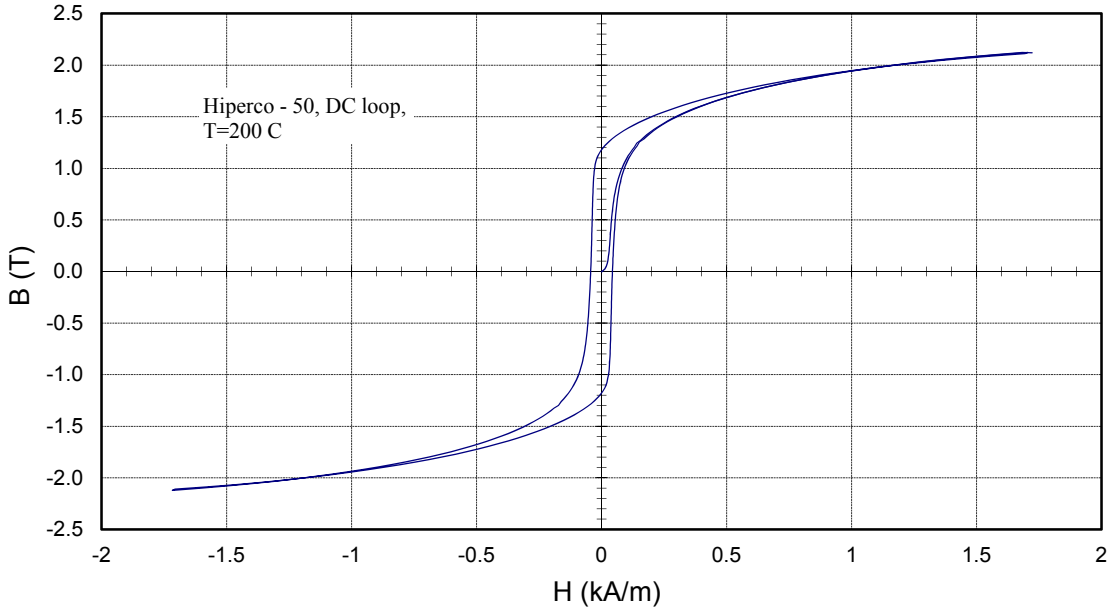

Figure 9.—Direct current BH properties of Hiperco 50 at 200 °C.

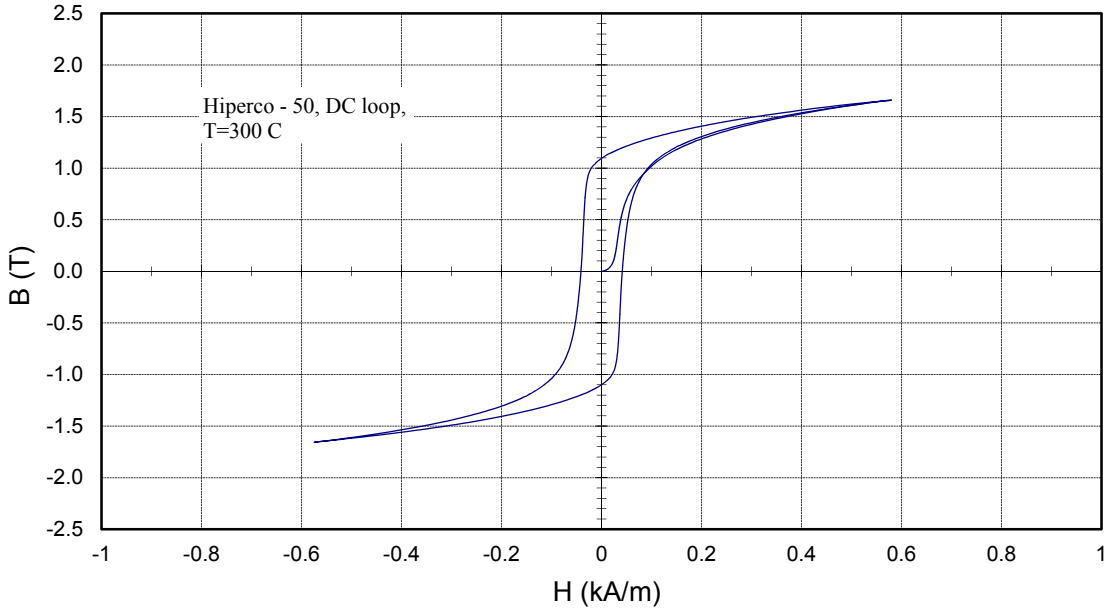

Figure 10.—Direct current BH properties of Hiperco 50 at 300 °C.

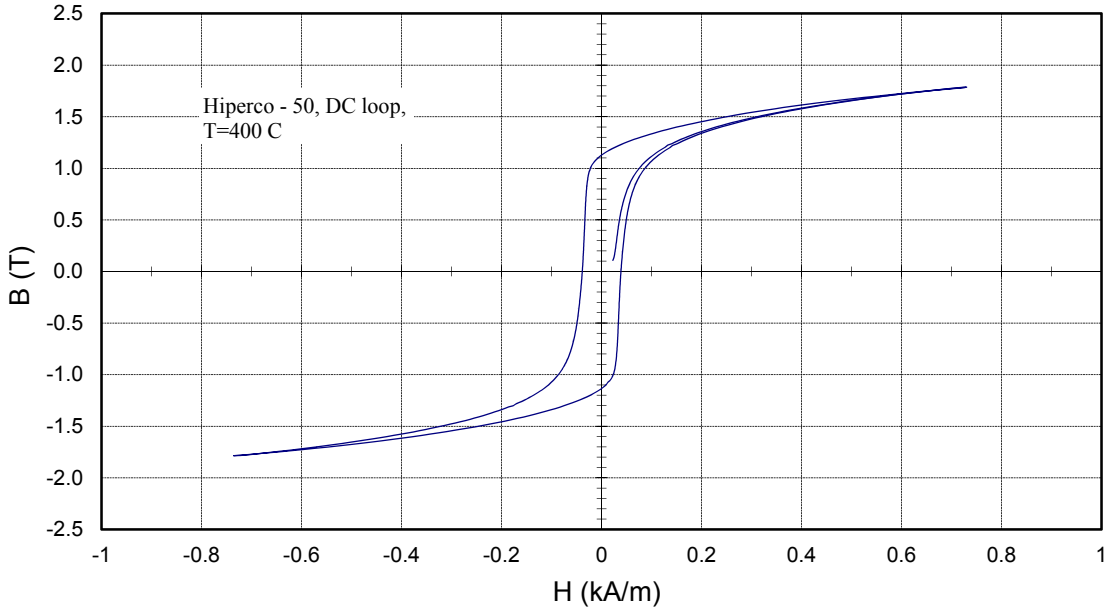

Figure 11.—Direct current BH properties of Hiperco 50 at 400 °C.

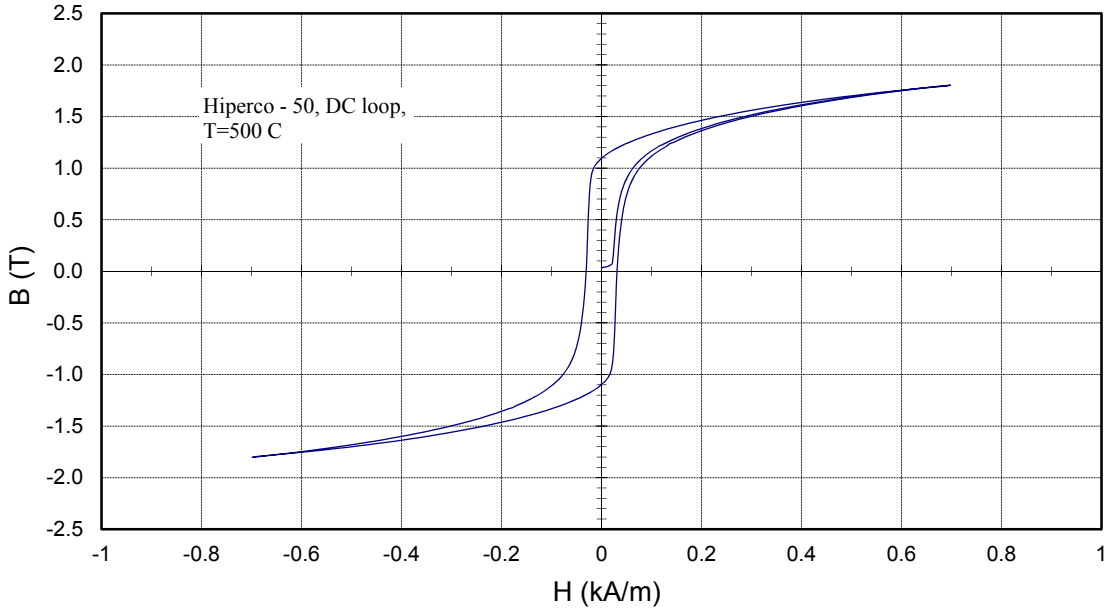

Figure 12.—Direct current BH properties of Hiperco 50 at 500 °C.

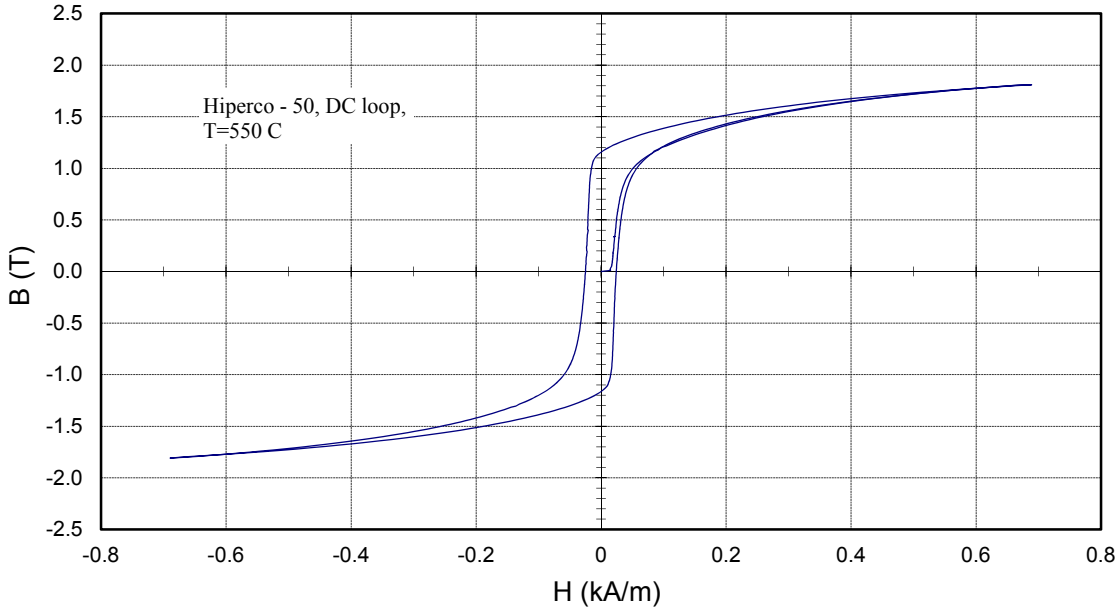

Figure 13.—Direct current BH properties of Hiperco 50 at 550 °C.

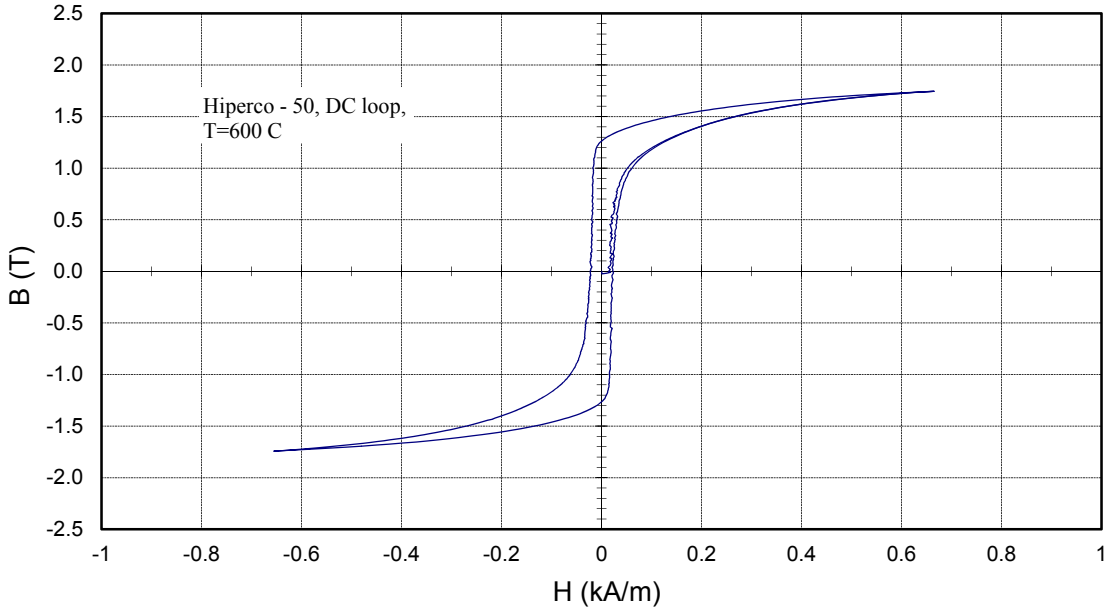

Figure 14.—Direct current BH properties of Hiperco 50 at 600 °C.

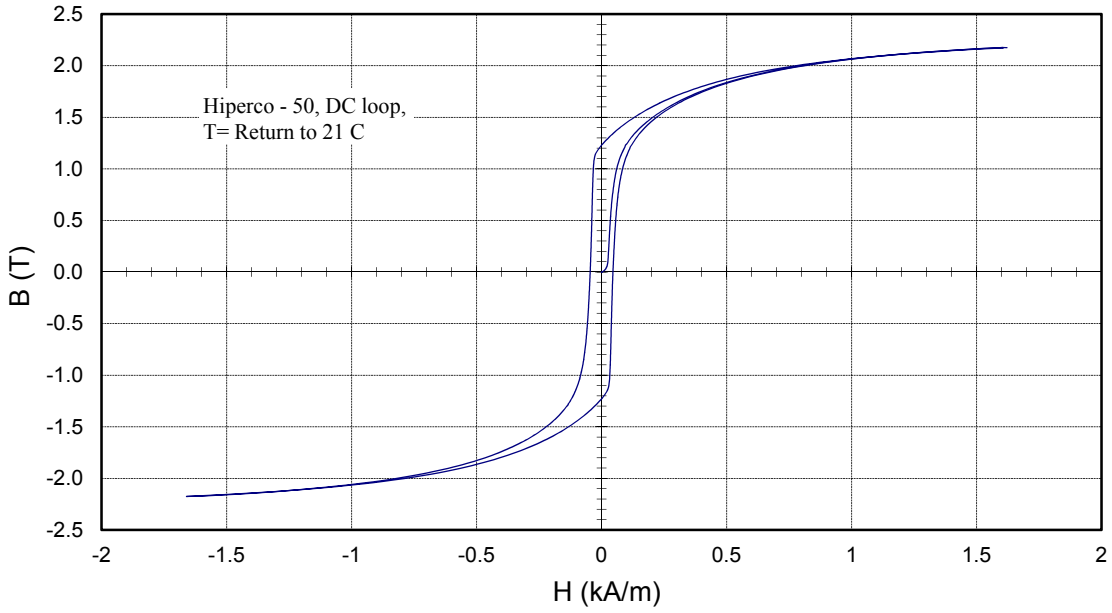

Figure 15.—Direct current BH properties of Hiperco 50 after returning to 23 °C.

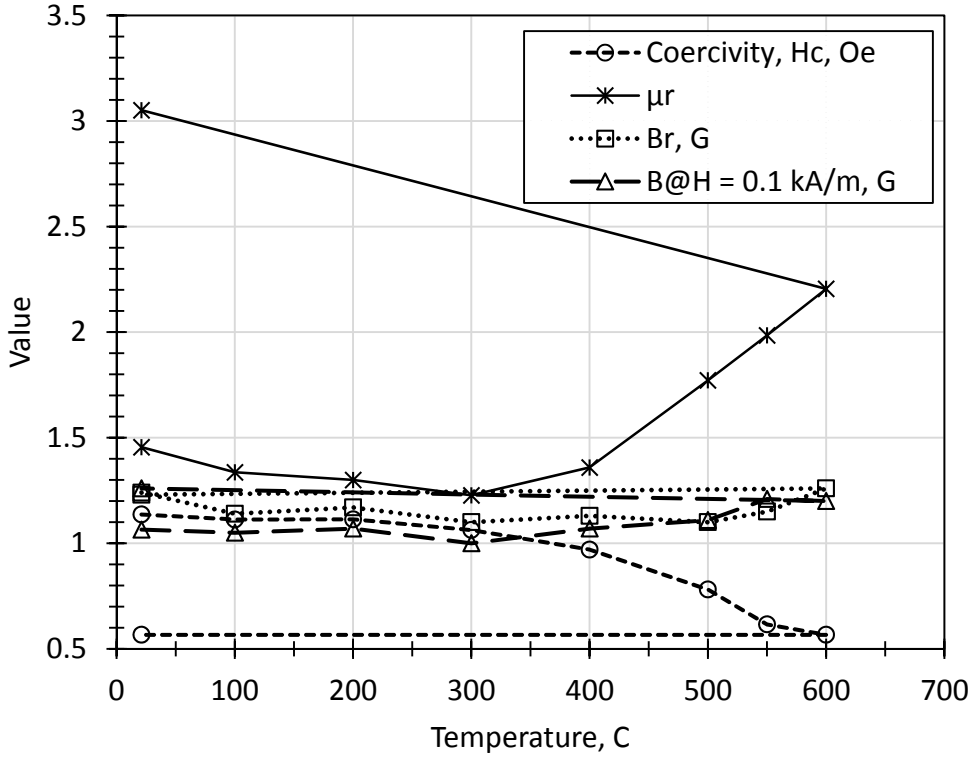

Figure 16.—Magnetic properties of Hiperco 50 at elevated temperatures; Units given in legend; Relative permeability (μr), Remanence (Br), and flux density B at H equals 0.1 kA/m are all multiplied by 10^{-4} (to get the value multiply by 10^{4}).

CMI-C Core Iron

Figure 17 compares the B-H curves for the Raw, Aged, and Annealed samples, each at 25 °C, to data extracted from FIG. X1.3 in Reference 20 for Class 1 low-carbon magnetic iron and a CMI-C sample recently tested after the following heat treatment: in H, heat to 850 °C with 4 h hold, heat to 1120 °C and hold for 4 h, 75 °C/h cooling to 550 °C followed by any non-quenching cooling to <200 °C. The magnetic performance of the raw sample is inferior to the annealed samples, as expected. The differences between the Aged and Annealed samples are within expected uncertainties for these measurements. This indicates that the low temperature and short time of the aging step did not significantly change the structure of the CMI-C sample. The Annealed and aged samples performed worse than the ASTM A848-01 standard for both Class 1 and Class 3 material; and worse than the CMI-C sample heat treated using the methods detailed in X3.3.2 in Reference 20.

Figure 18 compares the temperature dependence of the B-H curve for the Annealed sample at 25, 100, 200, 300, and 400 °C. At temperatures above 100 °C permeability decreased with increasing temperature; the approximate decline in the permeability at 400 °C compared to room temperature was 30% (as measured by the maximum slop between 0.1 and 1 kA/m). The saturation flux density, B_s was approximately equal for all temperatures below 400 °C. At 400 °C, the B-H curve flattens at values of H > 10 kA/m, thus resulting in lower B_s at 400 °C. Note that the sample is still substantially lower than the Curie temperature (770 °C (Ref. 33)).

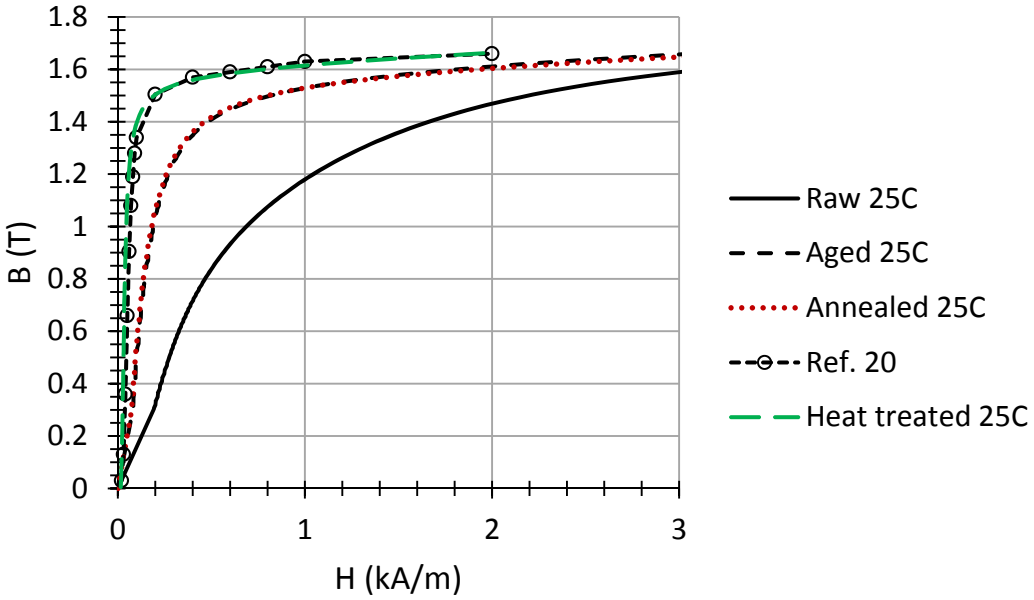

Figure 17.—B-H curve comparison of Raw, Aged, and Annealed samples to Class 1 A848 iron (Ref. 20) and a sample Heat treated differently, all tests were at room temperature.

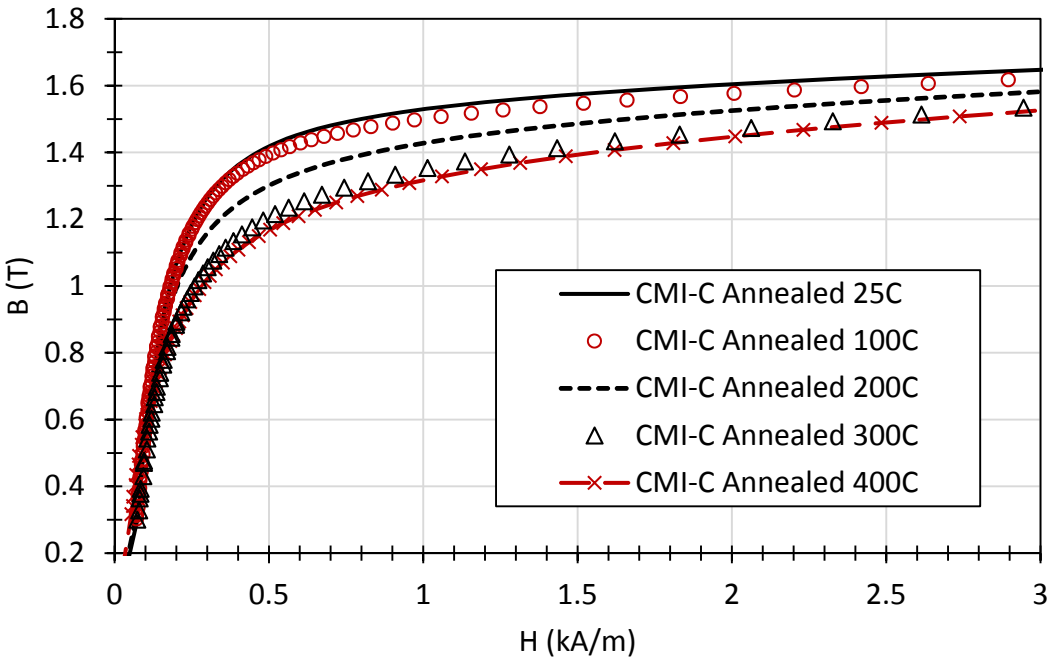

Figure 18.—B-H curves for the Annealed sample tested at various temperatures.

Conclusions

In a toroidal sample made from stacked thin sheets of Hiperco 50: coercivity decreased as test temperature increased, and remained low upon returning to room temperature, presumably due to grain growth as temperature increased. Permeability of the Hiperco 50 ring improved (increased) with increasing temperature and improved further upon returning to room temperature. It appears from the data that the grain structure and thus the magnetic properties of Hiperco 50 changed during elevated temperature testing. The larger grains were retained upon return to room temperature. The Barkhausen effect was observed in the initial magnetization curve at 600 °C.

The magnetic properties of the solid pure iron CMI-C ring samples did not improve at higher test temperatures but were improved by annealing (heat treating at 843 °C) and improved further by heat treating in a H atmosphere following ASTM A848-01, X3.3.2 recommendations. Iron samples were not significantly affected by aging at 204 °C for 4 h.

References

1. Fission Surface Power Team, “Fission Surface Power System Initial Concept Definition,” NASA/TM—2010-216772, NASA Glenn Research Center, Cleveland Ohio, 2010.
2. K.A. Polzin, J.B. Pearson, M.P. Schoenfeld, K. Webster, M.G. Houts, T.J. Godfroy, J.A. Bossard, “Performance Testing of a Prototypic Annular Linear Induction Pump for Fission Surface Power,” NASA/TP—2010-216430, Marshall Space Flight Center, Alabama, May 2010.
3. J.E. Dudenhoefer, J.M. Winter, D. Alger, “Progress Update of NASA’s Free-Piston Stirling Space Power Converter Technology Project,” NASA TM 105748, prepared for the NTSE Conference, American Nuclear Society, Jackson Hole, Wyoming, Aug., 1992.
4. W.A. Wong, J.G. Wood, K. Wilson, “Advanced Stirling Convertor (ASC)—From Technology Development to Future Flight Product,” NASA/TM—2008-215282, Dec. 2008, prepared for STAIF-2008, Albuquerque NM, Feb. 2008.

5. S.M. Geng, J.M. Niedra, K.A. Polzin, "Magnetic Analysis of an Annular Linear Induction Pump for Fission Power Systems," Nuclear and Emerging Technologies for Space, NETS 2012, March 2012, The Woodlands, TX, last retrieved 5/20/2015: http://www.lpi.usra.edu/meetings/nets2012/pdf/3033.pdf
6. R.H. Hofer, P.Y. Peterson, A.D. Gallimore, R.S. Jankovsky, "A High Specific Impulse Two-Stage Hall Thruster with Plasma Lens Focusing," Paper IEPC-01-036 presented at the 27th International Electric Propulsion Conference, Pasadena, CA, 15–19 October, 2001, Electric Rocket Propulsion Society.
7. R.S. Jankovsky, D.T. Jacobson, L.S. Mason, V.K. Rawlin, M.A. Mantenieks, D.H. Manzella, R.R. Hofer, P.Y. Peterson, "NASA's Hall Thruster Program," AIAA-2001-3888, 37th Joint Propulsion Conference, Salt Lake City, UT, July 8–11, 2001.
8. Carpenter Specialty Alloys, Technical Datasheet, Hiperco 50A Alloy, 2014, last retrieved Oct. 1, 2014, http://cartech.ides.com/datasheet.aspx?i=103&e=199&c=TechArt
9. G.W. Elmen, "Magnetic Alloys of Iron, Nickel, and Cobalt," Bell Sys. Tech. Jol., 1929.
10. J.K. Stanley and T.D. Yensen, Trans. AIEE, 66, 1947, p. 714.
11. Volume 2, FerroMagnetic Materials, a handbook on the properties of magnetically ordered substances, Edited by E.P. Wohlfarth, with the section on Fe-Co alloys attributed to G.Y. Chin and J.H. Wernick, North-Holland, Elsevier Sci. B.V., 1st ed. 1980, 2nd impression 1986, 3rd impression 1999, transferred to digital printing 2005, p. 168–178.
12. Physical Metallurgy, vol. 1, 4th edition, edited by R.W. Cahn, P. Haasen, Elsevier Sci., 1996, p. 268.
13. D.R. Thormburg, "High-Strength High-Ductility Cobolt-Iron Alloys," Jol. of Applied Phy., vol. 40, no. 3, 1969, pp. 1579–1580.
14. F. Zhu, X. Bi, et al., "Phase Transformation and magnetic properties of annealed Fe52.2Co46V1.8 alloy," Vacuum, 75, 2004, pp. 33–38.
15. T. Sourmail, "Evolution of strength and coercivity during annealing of FeCo based alloys," Scripta Mat. 51, 2004, pp. 589–591.
16. E. Josso, IEEE Trans. Mag. MAG-10, 1974, p. 161.
17. B. Thomas, Proc. Conf. 2nd EPS on Soft Magnetic Materials, Wolfson Cente for Magnetics Technology, Cardiff, Wales, 1975, p. 109.
18. ASTM Designation: A801 – 09, "Standard Specification of Wrought Iron-Cobalt High Magnetic Saturation Alloys (UNS R30005 and K92650), ASTM International, West Conshohocken PA.
19. L. Harner, Staff metallurgist for Ed Fagan Inc. personal communication regarding heat treatment for Hiperco 50A to optimize magnetic properties, 2015.
20. ASTM Designation: A848 – 01 (Reapproved 2011), "Standard Specification for Low-Carbon Magnetic Iron," ASTM International, West Conshohocken PA.
21. Certificate of Tests for VimVar Core Iron, Carpenter Technology Corporation Reading PA, 2010.
22. J. Bozzuto, President of CMI Specialty Products, personal communication regarding heat treatment for CMI-C to optimize magnetic properties, 2015.
23. J. Horwath, Z. Turgut, R. Fingers, "HIGH TEMPERATURE PROPERTIES AND AGING-STRESS RELATED CHANGES OF FeCo MATERIALS," AFRL-PR-WP-TR-2006-2176, July 2006, Air Force Research Laboratory, Wright-Patterson Air Force Base, Oh.
24. L. Li, "High temperature magnetic properties of 49%Co-2%V-Fe alloy," J. Appl. Phys. 79 (8), April 1996, p. 4578–4580.
25. P.E. Kueser, D.M. Pavlovic, D.H. Lane, J.J. Clark, M. Spewock, "Properties of Magnetic Materials for use in High-Temperature Space Power Systems," NASA SP-3043, NASA, Washington D.C., 1967, p. 126–130.
26. R.S. Sundar, S.C. Deevi, "Soft magnetic FeCo alloys: alloy development, processing, and properties," International Mat. Reviews vol. 50, no. 3, 2005, p. 157–192.
27. K.K. Bogma, Fiz. Met. Metalloved., 1966, 22, p. 148–151.
28. Metals Handbook, Desk Edition, edited by H.E. Boyer, T.L Gall, American Soc. for Metals, Metals Park Ohio, 1985, p. 20–1.

29. M. Morishita, N. Takahashi, D. Miyagi, M. Nakano, “Examination of Magnetic Properties of Several Magnetic Materials at High Temperatures,” PRZEGLĄD ELEKTROTECHNICZNY (Electrical Review), ISSN 0033-2097, R. 87 No 9b/2011, p. 106–110.
30. R.T. Fingers, R.P. Carr, Z. Turgut, “Effect of aging on magnetic properties of Hiperco 27, Hiperco 50, and Hiperco 50HS alloys,” Jol. of Applied Phy., vol. 91, no. 10, 2002, pp. 7848–7850.
31. J.M. Niedra and G.E. Schwarze, “Magnetization, Anomalous Barkhausen Effect, and Core Loss of Supermendur Under High Temperature Cycling,” IEEE Trans. on Mag7, vol. 4, December 1971.
32. H. Barkhausen, “Zwei mit Hilfe der neuen Verstarker entdeckte Erscheinugen,” (Two phenomena discovered with the help of the new amplifier) Physik Z. 20, 1919, p. 401–403.
33. Lee, E.W., *Magnetism: An Introductory Survey*, Dover Publications Inc, New York, 1970, p. 117.